Indian Journal of Chemical Technology
Vol. 30, May 2023, pp. 342-351
DOI: 10.56042/ijct.v30i3.70544

Evaluation of *Punica granatum* extract as an environmentally safe corrosion inhibitor for carbon steel in a solution of 1 M sulfuric acid

Mohamed E Elnagar[1], Hanaa M Elabbasy*[,2] & Abd El-Aziz S Fouda*[,3]
[1]PPG protective and marine coatings PMC, Egypt
[2]Misr Higher Institute for Engineering and Technology, Mansoura, Egypt
[3]Department Chemistry, Faculty of Science, Mansoura University, Mansoura-35516, Egypt
E-mail: asfouda@hotmail.com,helabbasy@hotmail.com

Received 15 January 2023; accepted 2 April 2023

In order to create an eco-friendly corrosion inhibitor *Punica granatum* extract (PG) was employed as the primary component for use in H_2SO_4 pickling procedures. The inhibition behaviour of C-steel in H_2SO_4 has been studied using weight-loss tests, polarization curves, electrochemical impedance spectroscopy, Fourier-transform infrared spectroscopy (FT-IR), and X-ray photoelectron spectroscopy (XPS).The outcomes demonstrate the extract's effective inhibition in 1 M H_2SO_4. Both an increase in concentration and temperature boosted the effectiveness of the inhibition. With the greater concentration of PG (300 ppm) and the higher applied temperature (45°C), the inhibition effectiveness reached 91.7%. Nevertheless, the inhibitory efficacy increased synergistically with the addition of potassium iodide, increasing from 81.5% to 95.0% at 25°C using the *weight-loss* technique. Adsorption on the C-steel caused the inhibitory effect, and this adsorption mechanism was compatible with the Temkin isotherm. According to the free energy of adsorption (ΔG^o_{ads} = 39.5 kJ/mol.), the PG extract adheres chemically to the surface of the C-steel. The efficient inhibitor *Punica granatum* (PG) extract may prevent corrosion of C-steel in H_2SO_4 solution.The extracts from *Punica granatum* (PG) are a commonly used green inhibitor that may be used to pickle metals.

Keywords: Adsorption, C-steel, *Punica granatum* extract, Sulfuric acid, Synergistic effect, Temkin isotherm

C-steel is alloy of iron that contains up to 2.1 % (as Weight %) carbon. C-steelis regarded as the most useful material because of its many manufacturing applications, great mechanical properties, and extremely low cost. In the metal finishing industry, acid solutions are frequently employed to reduce undesirable scale and corrosion, boiler cleaning, and heat exchangers[1-3]. Therefore, Inhibitors can eventually be used in the treatment process to prevent metal disintegration when using acids for cleaning[4]. Sulphuric acid is almost as frequently used for metal pickling as hydrochloric acid, but it does not evaporate, hence it is typically employed for pickling at high temperatures. The use of 1 M H_2SO_4 in our study is to ensure that the extract was completely dissolved. In fact, Organic compounds are most effectual corrosion inhibition with N, O and S atoms[5-6]. Because they are nontoxic and include phytochemical components, plant extracts are increasingly used to prevent corrosion in C-steel, as it considered an environmentally friendly corrosion inhibitor[7]. Plant extracts are an extremely abundant source of natural chemicals that may be handled inexpensively and are easily degraded in nature. Extract of Eucalyptus globulus Leaves[8], *Citrus sinensis*[9], *Artemisia judaica*[10], and Eucalyptus leaf[11], were investigated as C-steel corrosion retardants in H_2SO_4 media. *Punica granatum* (Pomegranate) (PG) extract is vastly used as a metal corrosion retardant in acidic media[12-16]. PG is commonly used in respiratory ailments, make tinctures, cosmetics, and other medical formulas[17]. PG is very abundant in ellagitannins which are high molecular weight water-soluble phenolic compounds. Ellagitannin hydrolysis generates hexahydroxy diphenic acid, which naturally rearranges into Ellagic acid (EA)[18,19]. EA is an incredibly thermodynamically stable molecule reflecting the four-ring lipophilic domain. The hydrophilic component is composed of four phenolic (hydroxyl) and two groupings of lactone (which can act as a donor or acceptor of the hydrogen bond). PG peels contain a significant number of such polyphenols as flavonoids attached to sugar, quercetin, kaempferol[20], flavonoid Di glycoside[21], organic acid[22] ellagic acid and ellagic tannin[23]. On the other hand, it was confirmed that steroid hormones like estrone[24], estradiol[25] and testosterone have also been found in PG extract[26]. Tannic acid (TA) is the standard hydrolysing tannin consisting of a combination of various gallic acid (GA) esters of glucose. TA occurs in barks and many plant fruits contain PG, chelates of iron due to their 10 galloyl groups and decreases non-heme iron intestinal absorption[27,28]. The targets of this study is to inspect the inhibitory impact of PG extract as an inexpensive, naturally occurring chemical that is also environmentally friendly, on the corrosion behavior of C-steel in 1 M H_2SO_4. In addition to using FT-IR and XPS analysis, the investigation is carried out using WL, PP, and EIS techniques.

Experimental Section

Preparation of C-steel and acid solution

The compositions of the C-steel samples used in the investigation are as follows: C (0.14), Cr (0.1), Ni (0.01), Si (0.0.024), Mn (0.5), P (0.05), S (0.05) as percent weight, and the remaining percent are for Fe. Mechanical polishing was performed on C-steel specimens with dimensions of (1.9 × 1.9 × 0.1) cm. Bidistilled water was used to clean the samples after they had been with emery paper of grades ranging from 250 to 1200. The surface was cleaned with acetone, and then it was dried using filter sheets. This preparation technique for specimens is referred to as the standard technique[29]. The 1 M H_2SO_4 solution (from analytical reagent grades), created by using bid stilled water for dilution, is the acid medium employed for this study.

Extraction of plant material

At room temperature, the PG plant product was dried in shade. Using electric mills finely ground and extracted using methanol for soaking. The solvent extract was isolated by rotary evaporation and vacuum-dried at 60-65°C. Ethanol (1 g/L) was used to liquefy the solid form of the extract. Until using, crude extracts had been refrigerated[30].

Weight loss (WL) method

In WL measurements, glass hooks were used to fully immerse the test specimens (that prepared as clear above) in a 100 mL volume of 1 M H_2SO_4 solution in the absence and at various PG extract concentrations (50–300 ppm). After a similar amount of time (30 to 180 min), samples were removed from the solution, rinsing them with bi-distilled water, drying them with filter paper, and weighing them once more. Three repetitions were given to each test to reduce the percentage of errors. The reduction in weight, ΔW (mg), of the C-steel specimens was measured using the specimens' weights before (W_1) and following being submerged in the acid solution (W_2) with the following relationship:

$$\Delta W = W_1 - W_2 \quad \ldots (1)$$

The corrosion rate (CR) of C-steel specimens was determined as follows[31]:

$$CR = \frac{\Delta W}{AT} \quad \ldots (2)$$

with A= surface area (cm^2) and t= time (min). The ΔW was used to compute surface coverage (Θ) and inhibitory effectiveness (% IE) by employing the following equation:

$$\%IE = 100 \times \theta = 100 \times 1 - \frac{\Delta W_{inh}}{\Delta W_{free}} \quad \ldots (3)$$

with ΔW_{free}= C-steel WL in 1 M H_2SO_4 without PG extract and ΔW_{free}= C-steel WL in 1 M H_2SO_4 with PG extract.

Techniques using electrochemistry

Three electrodes were set up in a glass cell to conduct electrochemical testing. First is the saturated calomel electrode (SCE) which serves as reference electrode, second is platinum counter electrode which serves as electrode auxiliary, and third is a square C-steel sample with a 1 cm^2 area which serves as working electrode. Since immersion of the electrode for 30 minutes in the test solution, all electrochemical measures at the OCP have been performed at 25°C. Electrochemical studies were produced by using the Potentiostat/Galvanostat, ZRA (PCI4-G750), DC105 and EIS300 Gamry instruments, which attaches to a computer in order to record and examine data using Echem analyst V.6.03.

Tests of potentiodynamic polarization (PP)

By applying a scan of 0.5 mV s^{-1} in the range of potential of -700 to +700 mV, we have achieved Tafel polarization plots with regard to the open circuit potential (E_{ocp}).There have been recorded both catholic and anodic polarization curves.For determining surface coverage (Θ) and percent inhibitory effectiveness (% IE), as seen below, the densities of the corrosive current (i_{corr}) without ($i_{corr(free)}$) and with ($i_{corr(inh)}$) PG extract were used[32].

$$\%IE = \theta \times 100 = \left[1 - \frac{i_{corr(inh)}}{i_{corr(free)}}\right] \times 100 \quad \ldots (4)$$

Electrochemical impedance spectroscopy (EIS) evaluations

In EIS tests, the potential of open circuit (OCP) and AC current signal of 10 mV peak to peak have been used between 100 kHz and 10 Hz in frequency. The amount of surface coverage (ϴ) and percent inhibitory effectiveness (% IE) can be computed by employing the following equation[33].

$$\%IE = \theta \times 100 = \left[1 - \frac{R_{ct(free)}}{R_{ct(inh)}}\right] \times 100 \qquad \dots (5)$$

with $R_{ct(free)}$= resistance of charge transfer without PG extract and $R_{ct(inh)}$= resistance of charge transfer with PG extract.

Surface examinations

Fourier-transform infrared spectroscopy (FT-IR) analysis

Technique of FTIR analysis is used to detect the functional groups of the inhibitor before and after metal immersion via peaks with certain values. The Attenuated Total Reflectance (ATR) method can be applied to examine the FTIR spectra of 300 ppm of PG extract in 1M H_2SO_4 prior to and following C-steel inundation for 24 h by apparatus of FTIR-spectrometer iS 10 (Thermo Fisher Scientific, United States of America).

X-ray photoelectron spectroscopy (XPS) analysis

Technique of XPS can be used to detect the interaction of the inhibitor with the metal by providing the adsorbed inhibitor atoms' energy spectra. After spending 24 h submerged in 1M H_2SO_4 solution containing 300 ppm of PG extract, the C-steel surface was subjected to an XPS analysis utilizing a device made by Thermo-Scientific in the United States of America called the ESCALAB 250Xi.

Result and Discussion

Measurements of WL

WL of C-steel was tested at 25 ±1°C after three hours of flood in 1M H_2SO_4 solution without and at different PG concentrations.It was known that as the extract concentration grew, its performance improved due to an increase in inhibitory efficiency and a decrease in CR. The increase in PG adsorption and surface coverage on C-steel surface as extract concentration grew may be the cause of the decreased CR[34]. The PG adsorbed layer isolates C-steel from acidic solutions and inhibits its corrosion[35].

Synergy impact

The C-steel CR in 1 M H_2SO_4 without and at different PG concentrations in the absence and presence of 1×10^{-2} M KI was tested at 25°C using the WL technique. The computed CR, θ and percent IE values were demonstrated in Table 1. According to the table's findings, the presence of KI promotes the lowering of C-steel CR values in 1 M H_2SO_4. The lowering in the rate of growth of corrosion with KI shows that the presence of KI boosts the extract inhibitory efficacy. Due to the increased surface coverage that brought about by adsorption of iodide ions by electrostatic interactions with PG extract, it was shown that KI considerably increased the inhibitory efficiency[36,37]. The synergistic parameter (S_I) was attained by applying the following equations[38-40].

$$S_I = \frac{1 - I_{1+2}}{1 - I'_{1+2}} \qquad \dots (6)$$

Table 1 — C-steel CR, θ, % IE and S_I in 1 M H_2SO_4 without and at different concentrations of PG in the absence and presence of 1×10^{-2} M KI at 25°C

Conc. of KI(M)	Extract Conc.(ppm)	CR (mg cm^{-2} min^{-1})	ϴ	%IE	S_I
	Blank	0.412	—	—	—
	50	0.136	0.669	66.9	—
	100	0.112	0.669	66.9	—
	150	0.104	0.748	74.8	—
	200	0.097	0.764	76.4	—
	250	0.089	0.784	78.4	—
	300	0.076	0.815	81.5	—
$1x\ 10^{-2}$	Blank	0.052	0.873	87.3	—
	50	0.049	0.882	88.2	0.356
	100	0.028	0.933	93.3	0.516
	150	0.023	0.944	94.4	0.572
	200	0.021	0.950	95.0	0.599
	250	0.021	0.949	94.9	0.538
	300	0.021	0.950	95.0	0.470

$$I_{1+2} = I_1 + I_2 \quad \ldots (7)$$

with I_1 to express the inhibitory effectiveness of the anion, I_2 to express the inhibitory effectiveness of the captions, and I'_{1+2} toexpress the inhibitory effectiveness of both the captions and anion. The determined synergistic parameter (S_I) was tabulated in Table 1. When S_I approaches unity, the inhibitor molecules do not interact, when S_I exceed one denotes a synergistic impact, and when S_I falls below one, it signifies the emergence of a competitive adsorption[41]. The obtained $S_I$falls below one, thus it denotes competitive adsorption behaviour of PG extract and iodide ions. Data show that when potassium iodide is added, CR decreases, which increases the absorption of PG extract in the existence of potassium iodide[42].

Effect of temperature and thermodynamic parameters

Weight loss method results (CR, Θ and % IE) at different concentrations of PG extract at the applied temperatures (25- 45°C) for C-steel in 1M H_2SO_4 were shown in Table 2. It is obvious that by increasing the temperature, the extract inhibitory effectiveness increases, this implies that more extract molecules have stronger adsorptive interactions with C-steel/solution interface at higher temperature. This producing a protective layer of the inhibitor on the surface of the metal prohibits corrosion. An increase in the extract inhibitory effectiveness as temperature rises is a sign that the extract species have chemically adsorbed to the surface of the C-steel.

Table 2 — WL method results (CR, Θ and % IE) for C-steel without and at different concentrations of PG at different temperatures (25-45°C)

Temp (°C)	Extract conc.(ppm)	C.R	Θ	% IE
25	Blank	0.412	—	----
	50	0.136	0.670	67.0
	100	0.112	0.728	72.8
	150	0.104	0.748	74.8
	200	0.097	0.765	76.5
	250	0.089	0.784	78.4
	300	0.076	0.816	81.6
30	Blank	0.443	—	—
	50	0.140	0.684	68.4
	100	0.122	0.725	72.5
	150	0.107	0.758	75.8
	200	0.106	0.761	76.1
	250	0.098	0.779	77.9
	300	0.076	0.827	82.7
35	Blank	1.080	—	—
	50	0.279	0.742	74.2
	100	0.256	0.763	76.3
	150	0.229	0.788	78.8
	200	0.212	0.804	80.4
	250	0.182	0.831	83.1
	300	0.134	0.876	87.6
40	Blank	1.568	—	—
	50	0.371	0.763	76.3
	100	0.320	0.796	79.6
	150	0.302	0.807	80.7
	200	0.268	0.829	82.9
	250	0.231	0.852	85.2
	300	0.169	0.892	89.2
45	Blank	1.854	—	—
	50	0.387	0.791	79.1
	100	0.325	0.825	82.5
	150	0.258	0.861	86.1
	200	0.250	0.865	86.5
	250	0.236	0.873	87.3
	300	0.152	0.917	91.7

The corrosion process activation energy (E_a^*) can be attained by applying the Arrhenius equation as shown below:

$$\log\ CR = [\log\ A] - \left[\frac{E_a{}^*}{2.303\ R\ T}\right] \quad \ldots(8)$$

with R= universal gas constant (8.314 Joule/ mol. K), A is Arrhenius pre-exponential multiplier. Figure 1 indicates plot between log CR and 1/T for C-steel in 1 M H_2SO_4 without and at different PG extract concentrations. The E_a^* value could be gotten from the straight lines slopes. Another type of transition state expression can be employed to attain the enthalpy (ΔH^*) and the entropy (ΔS^*) of the activation mechanism as indicated below[43]:

$$CR = \left[\frac{RT}{Nh}\right] \exp\left[\frac{\Delta S^*}{R}\right] \exp\left[\frac{-\Delta H^*}{RT}\right] \quad \ldots(9)$$

with h and N as constant of Planck and number of Avogadro, respectively. Straight lines were attained from the graphs of (1/T) and (log CR/T) (Fig. 2). From the slopes and intercepts of the lines, ΔH^* and ΔS^* can be obtained, respectively. The attained E_a^*, ΔH^* and ΔH^* parameters were given in Table 3. It was found out that the inhibited solutions' E_a^* values are lower than that for a blank solution. The decrease in E_a^* indicates that the PG particles have chemisorbed onto C-steel surface. ΔH^* indicates that the activation mechanism is endothermic through its positive sign. The lower values of ΔH* in inhibited solutions compared to a blank solution, implies that the corrosion reaction energy barrier is lowered. The negative values of ΔS^* points out that association occurs in the activated complex rather than dissociation, in other words, the change from the reactant until the activated complex includes a decrease in the disorder[44,45].

Adsorption isotherm

To acquire essential crucial data regarding the corrosion inhibition process, adsorption isotherms might be used. Numerous adsorption isotherms were tested, and Temkin isotherm, which agrees with the following equation, was the best one.

$$a\theta = \ln K_{ads} C \quad \ldots (10)$$

where C= concentration of extract, a= the attractive parameters and K_{ads}=adsorption constant. Plots of

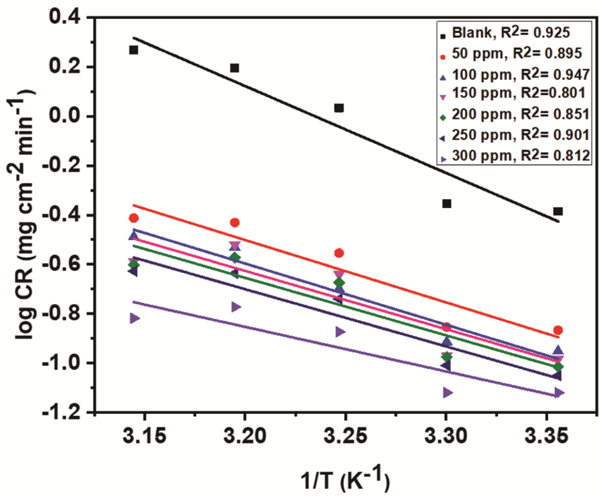

Fig. 1 — Graphs of log CR against 1000/T for C-steel in 1 M H_2SO_4 without and at different PG extract concentrations.

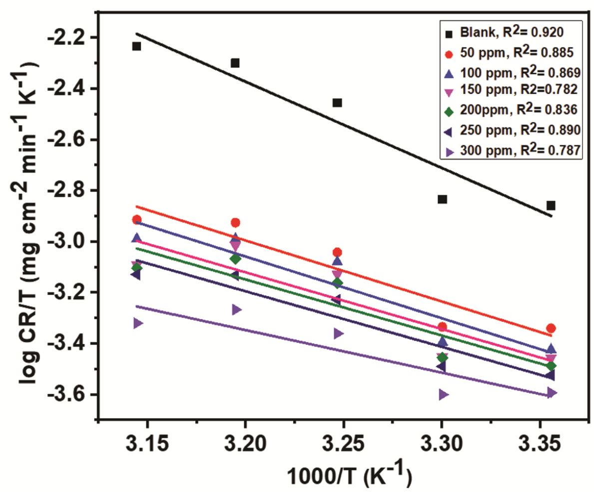

Fig. 2 — Graphs of log CR/T against 1000/T for C-steel in 1 M H_2SO_4 without and at different PG extract concentrations.

Table 3 — Thermodynamic activation parameters for C-steel without and at different PG extract concentrations in 1 M H_2SO_4 solution

Extract conc, (ppm)	E_a^*, (kJmol^{-1})	ΔH^*, (kJ mol^{-1})	$-\Delta S^*$, (J mol^{-1} K^{-1})
Blank	67.4	64.8	35.5
50	48.4	45.8	108.2
100	47.5	46.3	107.7
150	45.2	42.6	120.8
200	44.6	42.1	123.1
250	44.4	41.8	124.9
300	34.6	32.0	159.2

Temkin isotherm appears in Fig. 3. It is possible to acquire the free adsorption energy (ΔG^{o}_{ads}) by applying the following equation:

$$K_{ads} = \frac{1}{55.5} \exp \frac{-\Delta G^{o}_{ads}}{RT} \quad \text{... (11)}$$

with 55.5 as the molarity of water in the solution. Van't Hoff plot (Fig. 4) is a simple way to both qualitatively and quantitatively measure the enthalpy of the adsorption process (ΔH^{o}_{ads}), according to the following equation[46]:

$$\log K_{ads} = \frac{-\Delta H^{o}_{ads}}{2.303RT} + \text{constant} \quad \text{... (12)}$$

Using the fundamental thermodynamic principle equation, the entropy of adsorption (ΔS^{o}_{ads}) may be determined as follows:

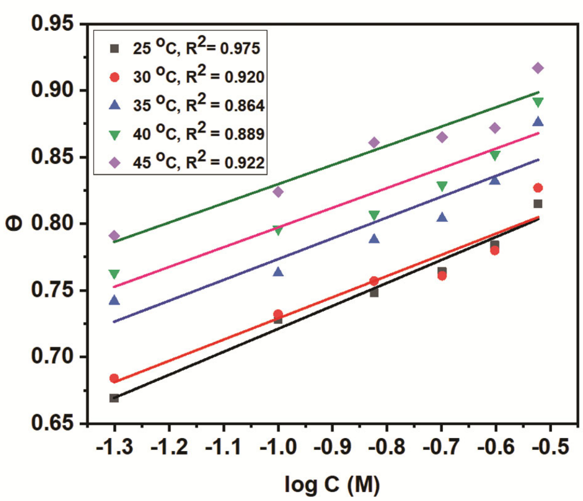

Fig. 3 — Temkin model of PG extract adsorption on C-steel surface at various temperatures.

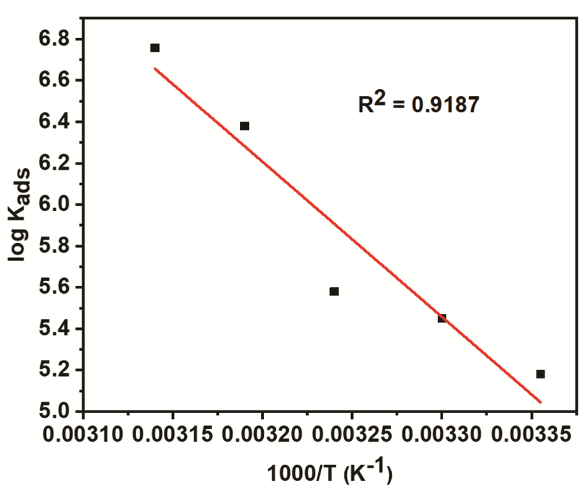

Fig. 4 — Graph of log K_{ads} and 1/T for the PG adsorption on the surface of C-steel.

$$\Delta S^{o}_{ads} = \frac{\Delta H^{o}_{ads} - \Delta G^{o}_{ads}}{T} \quad \text{... (13)}$$

Table 4 described the received adsorption parameters. The values of ΔG^{o}_{ads} are negative and grew as the percentage IE rose, indicating that the studied extract is heavily adsorbed on the surface of C-steel. These results further demonstrate the spontaneity of the adsorption process and the stability of the adsorbed layer on surface of the C-steel[47]. The values of ΔG^{o}_{ads} obtained were greater than 40 kJ mol^{-1}, supporting chemisorptions as the mode of the extract adsorption on the surface of the metal[48]. The K_{ads} follows the similar pattern in that higher K_{ads} values indicate better, more effective adsorption and, hence, stronger inhibitory effectiveness. The extract adsorption from a 1 M H_2SO_4 solution onto the surface of C-steel is revealed to be an exothermic process by the negative sign of the ΔH^{o}_{ads} equation, which means that the extract %IE rises as the temperature grew. Such attitude can be discussed by the reality that as temperature grows, more inhibitor molecules adsorbed onto the metal's surface, leading to the observation of higher protection. It was shown that the entropy of adsorption (ΔS^{o}_{ads}) exhibits negative indicators, indicating that the disorder is diminished in conjunction with the adsorption process.

Electrochemical measurements

Tests of potentiodynamic polarization (PP)

The potentiodynamic curvesforC-steel in 1 M H_2SO_4 without and with PG extract at 25°C are seen in Fig. 5. Polarization measurements can be used to determine cathodic and anodic Tafel slopes (β_c and β_a), corrosion potential (E_{corr}), corrosion current density (i_{corr}), percent inhibitory effectiveness (%IE) and extent of surface coverage (θ). The computed PP data are presented in Table 5. It is obvious that the PG extract presence reduces i_{corr}, which is caused by the extract molecules adsorption onto the C-steel surface. In the E_{corr} and Tafel slopes, there is little difference between

Table 4 — Parameters of adsorption of PG extract on the surface of C-steel at different temperatures.

Temp (°C)	a	log K_{ads}	$-\Delta G_{ads,}$ (kJ mol^{-1})	$-\Delta H_{ads,}$ (kJ mol^{-1})	$-\Delta S_{ads,}$ (J mol^{-1} K^{-1})
25	13.36	5.18	39.5		614.4
30	13.97	5.45	41.7		611.6
35	14.75	5.58	43.2	143.6	606.5
40	15.53	6.38	48.6		614.1
45	15.98	6.76	51.7		614.2

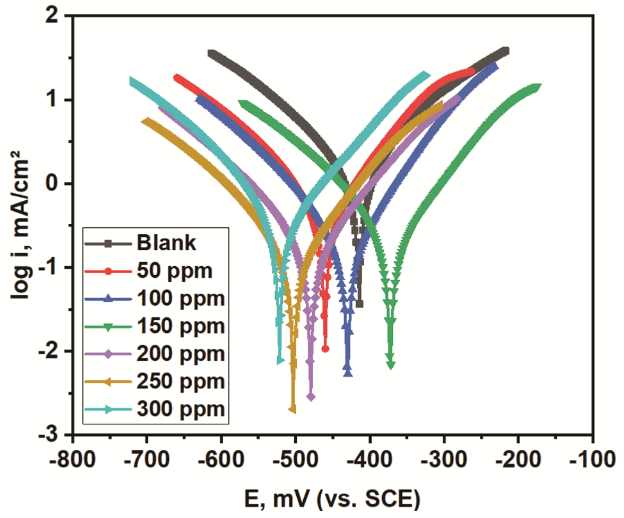

Fig. 5—Anodic and cathodic PP curves for C-steel in 1 M H_2SO_4 without and at PG concentration at 25°C.

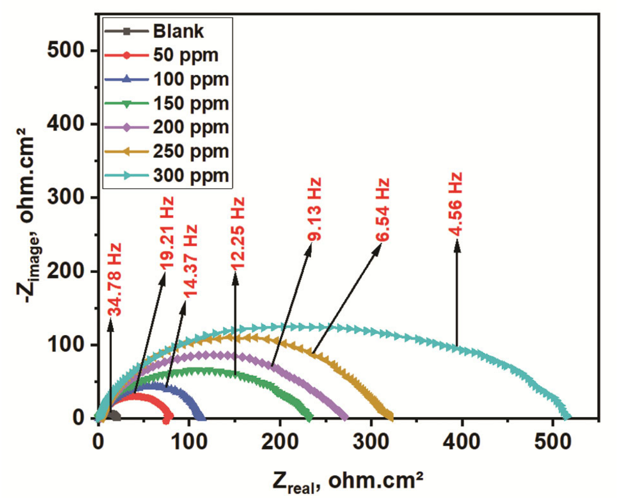

Fig. 6 — Nyquist charts for C-steel in 1 M H_2SO_4 without and at different PG extract concentrations.

the uninhibited and inhibited solutions. The existence of the tested extract did not significantly change the E_{corr} values, proving the inhibitor's ability to act as a mixed type inhibitor[49]. Additionally, it was noticed that Tafel lines shifted the cathodic (β_c) and anodic (β_a) slopes in more negative and positive orientations, respectively, demonstrating that the corrosion reaction process is established and the straightforward adsorption strategy prevents the corrosion reaction[50].

Tests of electrochemical impedance spectroscopy (EIS)

In corrosion studies, EIS is an effective and useful method. A lot of details can be obtained from impedance diagrams, such as kinetic parameters, surface properties, and mechanistic information[51-53]. The Nyquist charts for

Table 5 — Effect of PG concentration on PP parameters for C-steel in 1 M H_2SO_4 at 25°C

Extract conc., (ppm)	$-E_{corr}$, (mV)	i_{corr}, (mA cm^{-2})	β_a, (mV dec^{-1})	$-\beta_c$, (mV dec^{-1})	Θ	%IE
Blank	414.8	0.9430	122.5	139.2	—	—
50	460.7	0.5102	128.4	156.6	0.459	45.9
100	429.5	0.4039	97.1	126.9	0.572	57.2
150	372.7	0.3171	118.8	142.2	0.664	66.4
200	479.1	0.1949	123.8	137.0	0.793	79.3
250	503.2	0.1183	121.7	143.8	0.875	87.5
300	394.3	0.0484	157.9	166.9	0.949	94.9

Table 6 — EIS parameters for C-steel in 1 M H_2SO_4 without and at different PG extract concentrations

Extract conc., (ppm)	R_s, (Ω cm^2)	n	C_{dl}, (µF cm^{-2})	R_{ct}, (Ω cm^2)	Θ	%IE
Blank	2.521	0.985	608.7	25.12	—	—
50	3.605	0.992	437.4	60.24	0.580	58.3
100	1.905	0.989	384.5	87.48	0.713	71.3
150	3.338	0.994	296.4	143.13	0.824	82.4
200	3.481	0.955	208.3	197.7	0.873	87.3
250	3.879	0.911	145.7	302.6	0.917	91.7
300	4.048	0.972	65.31	516.1	0.951	95.1

C-steel in 1 M H_2SO_4 at 25°C were displayed in Fig. 6 at open-circuit potential without and at different PG extract concentrations. The results indicate an expansion of the Nyquist plot semicircle diameter when the extract concentration boosts from 50 to 300 ppm. Equivalent circuit model was applied to fit EIS results. It consists from the charge transfer resistance (R_{ct}), the phase element component (CPE) and solution resistance (R_s). The CPE was used in the place of double layer capacitance (C_{dl}) for better fitting. Different EIS parameters were computed and included in Table 6. It found that there is a growth in (R_{ct}) values while there was a gradually drop in (C_{dl}) values as concentration of PG increases. This may be a result of the extract gradually replacing molecules of water through the adsorption on the metal surface or a result of thickening the double layer. As indicated in Table 6, n values have range of (0.985-0.972). The deviation from unity can be illustrated on the bases of heterogeneity and roughnessthat appeared on the C-steel surface[54].

Surface examinations

Analysis of Fourier-transform infrared spectroscopy (FT-IR)

FT-IR method identified specific peaks in the extract IR spectra that corresponded to the functional groups[55]. The FT-IR spectra of the PG extract prior to and following C-steel immersion was studied. The large peaks were noted at (3328 cm^{-1}) for O-H, (2975 cm^{-1})

Table 7 — Peak BE (eV) of the core elements for C-steel after inundation in 1 M H_2SO_4 with 300 ppm of PG extract for 24 h

Core element	Peak BE,(eV)	Assignments
C1s	284.89	C-C, C-H
	288.7	
	286.5	C-$^{+}$O, C-S, C=N, C-$^{+}$N, C=O
	287.08	
Fe2p	712.47	
	727.19	
	720.34	Metallic iron
	714.31	$Fe2p_{1/2}$ of Fe^{3+}
	730.63	$Fe2p_{3/2}$
	733.77	$Fe2p_{1/2}$of Fe^{3+}
	710.77	Satellite of Fe^{3+}
	724.4	$Fe2p_{1/2}$ of Fe^{2+}
	717.87	
N1s	399.99	
	400.18	neutral imine (-N=) andamine (-N-H)
	401.89	
O1s	532.43	
	530.13	Metal oxide, Hydroxide, FeO and Fe_2O_3
	533.08	
S2p	169.46	Sulfide and sulphite
	168.48	

for aliphatic C-H stretching vibration frequencies, (1718 cm^{-1}) for C-O symmetric stretch, (1613 cm^{-1}) for C=O, and (1343 cm^{-1}) for C-H. Between the spectra of the extract in 1M H_2SO_4 before and after C-steel inundation, it is evident that some peaks migrate or vanish, and other peaks become less prominent. These peaks changes show how the C-steel surface interacts with the PG extract molecules[56]. This implies that the extract was adsorbed onto the metal surface via the molecules functional group, leding to the inhibition process.

Analysis of X-ray photoelectron spectroscopy (XPS)

The XPS spectra of the primary components found in the layer generated on the surface of C-steel following exposure to an acid media containing a greater concentration of PG extract (300 ppm). The peak binding energies (BE, eV) are shown in Table 7 along with the corresponding assignment[57-65]. The (-N =) and (-N-H) can be identified by three peaks in the N1s spectra at 400.23 eV, 401.89 eV, and 399.99 eV, respectively. The S2p spectra also showed two peaks at energies of 168.48, 169.46, and 166.9 eV, which correspond to adsorbed S on C-steel. Four unique peaks were also seen in the C1s spectra at (284.63 eV) for (C-C, C-H), and (286.6 eV, 288.79 eV, and 287.08 eV) which indicate (C-+O, C-S, C=N, C-+N, C=O). Moreover, three distinct peaks in the O1s spectrum with 530.13, 532.43.01, and 533.08 eV, which associated with metal oxide, hydroxide, ferrous oxide, and ferric oxide. The XPS examination results support adsorption of the PG extract on C-steel surface in an acidic solution.

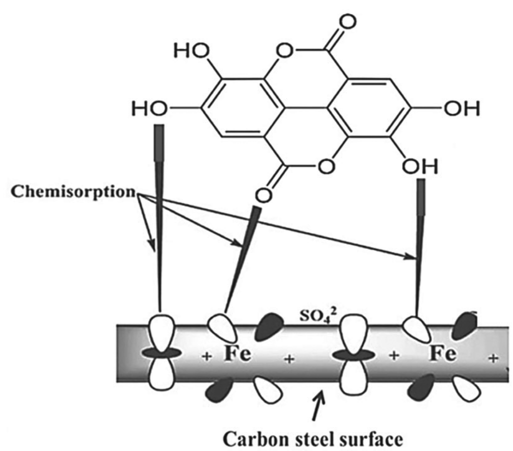

Scheme 1 — Explanation of adsorption mechanism of the Ellagic acid molecule of PG extract as example on the surface of C-steel.

Inhibition mechanism

It's crucial to assess the experimental and calculated data in order to understand the inhibitory mechanism of PG in 1 M H_2SO_4. The investigated PG extract contains numerous compounds with a lot of heteroatoms and aromatic rings operate as Lewis bases. These compounds create coordination bonds with Fe's free d-orbital, and act as a barrier contra surroundings that causing corrosion. Scheme 1 shows explanation of the adsorption mechanism of the Ellagic acid molecule of PG extract on the surface of C-steel.

Conclusions

In a solution of 1 M H_2SO_4, the PG extract seems to have a strong inhibitory efficiency for C-steel corrosion and the process of inhibition was fundamentally elucidated by the adsorption. PG extract adsorption on a surface of C-steel followed the Temkin adsorption isotherm. The adsorption is chemisorptions. The percentage of IE rises with increased extract dosage and increased temperature. The statistics of the synergistic effect show a decrease in CR when we add KI, and this due to the increase in the absorption of PG extract in the presence of potassium iodide. According to PP procedures, PG extract has cathodic and anodic inhibitory effects. Increasing PG extract causes a decrease in C_{dl} while achieving an increase in R_{ct}. Results from FT-IR and XPS for C-steel surfaces with PG show that an inhibitive film forms on the surface of C-steel, preventing its corrosion in 1M H_2SO_4 solutions.

References

1 Chauhan L R & Gunasekaran G G, *Corro Sci*, 49 (2007) 1143.
2 Lalitha A, Ramesh S & Rajeswari S, *Electro chim Acta*, 51 (2005) 47.
3 Quraishi M A & Sardar R, *Corros*, 28 (2002) 103.
4 Sykes J M, *Br Corros J*, 25 (1990) 175.
5 Elkadi L, Mernari B, Traisnel M, Bentiss F & Lagrenee M, *Corros Sci*, 42 (2000) 703.
6 Schmitt G, *Br Corros J*, 19 (1984) 165.
7 Raja P B & Sethuraman M G, *Mater Lett*, 62 (2008) 113.
8 Tezeghdenti M, Dhouibi L & Etteye N, *J Bio Tribo Corros*, 1 (2015) 5.
9 Ali A E, Badr G E & Fouda A S, *Biointerface Res Appl Chem*, 11 (2021) 14007.
10 Fouda A S, Shalabi K & Alsadeag A, *Int J Petrochem Sci Eng*, 2 (2017) 228.
11 Abdal-nabi S M & Mahdi S M, *Int J Mech Eng Educ*, 7 (2022) 2247.
12 Chidiebere M A, Ogukwe C E, Oguzie K L, Eneh C N & Oguzie E E, *Ind Eng Chem Res*, 51 (2012) 668.
13 Sorkhabi H A, Mirzaee S, Rostamikia T & Bagheri R, *Int J Corros*, 2015 (2015) 1.
14 Sahraoui M, Boulkroune M, Chibani A, Larbah Y & Abdessemed A, *J Bio Tribo Corros*, 8 (2022) 54.
15 Cheyad M S & Salman T A, *J Mater Sci Sur Eng*, 5 (2017) 597.
16 Rani P D & Selvaraj S, *J Phytol*, 2 (2010) 58.
17 Negi P S, Jayaprakasha G K & Jena B S, *Food Chem*, 80 (2003) 393.
18 Komorsky-Lovrić Š & Novak I, *Int J Electrochem Sci*, 6 (2011) 4638.
19 Häkkinen S H, Kärenlampi S O, Mykkänen H M & Heinonen I M, Törrönen A R, *Food Res Technol*, 212 (2000) 75.
20 Chauhan D & Chauhan J S, *Pharm Biol*, 39 (2001) 155.
21 El-Toumy S A & Rauwald H W, *Phytochem*, 61 (2002) 971.
22 Heftmann E, Ko S T & Bennett R D, *Phytochem*, 5 (1966) 1337.
23 Poyrazoğlu E, Gökmen V & Artık N, *J Food Compos Anal*, 15 (2002) 567.
24 Dean P, Exley D & Goodwin T, *Steroid in plants: Re-estimation of oestrone in pomegranate seeds*, (1971).
25 Wahab S, Fiki N, Mostafa S & Hassan A, *Bull Fac Pharm Cairo Univ*, 36 (1998) 11.
26 Choi D W, Kim J Y, Choi S H, Jung H S, Kim H J, Cho S Y & Chang S Y, *Food Chem*, 96 (2006) 562.
27 Brune M, Rossander L & Hallberg L, *Eur J Clin Nutr*, 43 (1989) 547.
28 Geisser P, *Arzneim Forsch*, 40 (1990) 754.
29 ASTM, AST G 31-72, Standard Recommended Practice for the Laboratory Immersion Corrosion Testing of Metals, American Society for Testing and Materials, Philadelphia, PA, USA, (1990).
30 Lecante A, Robert F, Blandinières P A & Roos C, *Curr Appl Phys,* 11 (2011) 714.
31 Barsoukov E & Macdonald J R, *Impedance Spectroscopy, Theory, Experiment and Applications*, 2nd edn Wiley Inter-science publications, New York, (2005).
32 Emori W, Zhang R H, Okafor P C, Zheng X W, He T, Wei K, Lin X Z & Cheng C R, *Colloids Surf A Physicochem Eng Asp*, 290 (2020) 124534.
33 Akinbulumo O A, Odejobi O J & Odekanle E L, *Results Mater*, 5 (2020) 100074.
34 Fouda A S, Shalabi K, Nofal A M & El-Zekred M A, *Chem Sci Trans*, 7 (2018) 101.
35 Toghan Arafat, Gadow H S, Dardeer H M & Elabbasy H M, *J Mol Liq*, 325 (2021) 115136.
36 Elabbasy H M & Gadow H S, *J Mol Liq*, 321 (2021) 114918
37 Gerengi H, Ugras H I, Solomon M M, Umoren S A, Kurtay M & Atar N, *J Adhes Sci Technol*, 30 (2016) 2383.
38 Usman B J, Umoren S A & Gasem Z M, *J Mol Liq*, 237 (2017) 146.
39 Zhang Z, Tian N, Zhang W, Huang X, Ruan L & Wu L, *Corros Sci*, 111 (2016) 675.
40 Pavithra M K, Venkatesha T V, Vathsala K & Nayana K O, *Corros Sci*, 52 (2010) 3811.
41 Djellab M, Bentrah H, Chala A & Taoui H, *Mater Corros*, 70 (2019) 149.
42 Yan Y, Li W, Cai L & Hou B, *Electrochim Acta*, 53 (2008) 5953.
43 Mazkour A, El Hajjaji S, Labjar N, Lotfi E & El Mahi M, *Int J Corros,* 2021 (2021) 6666811.
44 Şafak S, Duran B, Yurt A & Türkoğlu G, *Corros Sci*, 54 (2012) 251.
45 Fouda A S, Megahed H E, Fouad N & Elbahrawi N M, *J Bio Tribo Corros*, 2 (2016) 1.
46 Al-Amiery A A, Kadhum A H, Alobaidy A H M, Mohamad A B & Hoon P S, *Materials (Basel)*, 7 (2014) 662.
47 Elabbasy H M & Fouda A S, *Green Chem Lett Rev*, 12 (2019) 332.
48 Heakal F E, Deyab M A, Osman M M, Nessim M I & Elkholy A E, *RSC Adv*, 7 (2017) 47335.
49 Ajmal M, Mideen A S & Quraishi M A, *Corros Sci*, 36 (1994) 79.

50 Bentiss F, Lebrini M & Lagrenee M, *Corros Sci*, 47 (2005) 2915.

51 Silverman D C & Carrico J E, *Corros*, 44 (1988) 280.

52 Macdonald D D & McKubre M C, Impedance measurements in electrochemical systems, *Mod Asp Electrochem*, Springer, Boston, MA. (1982) 61.

53 Mansfeld F, *Corros*, 37 (1981) 301.

54 Solmaz R, Kardas G, Ulha M C, Yazıcı B & Erbil M, *Electrochim Acta*, 53 (2008) 5941.

55 Fouda A S, Mohamed O A & Elabbasy H M, *J Bio Tribo Corros*, 7 (2021) 135.

56 Khadom A A, Abd N A & Ahmed N A, *S Afr J Chem Eng*, 25 (2018) 13.

57 Hashim N Z N, Anouar E, Kassim K, Zaki H M, Alharthi A I & Embong Z, *Appl Surf Sci*, 476 *(*2019) 861.

58 Meneguzzi A, Ferreira C, Pham M C, Delamar M & Lacaze P C, *Electrochim Acta*, 44 (1999) 2149.

59 Lebrini M, Lagrene´e M, Traisnel M, Gengembre L, Vezin H & Bentiss F, *Appl Surf Sci*, 253 (2007) 9267.

60 Eid A M, Shaaban S & Shalabi K, *J Mol Liq*, 298 (2020) 111980.

61 Moulder J F, Stickle W F, Sobol P E & Bomben K D, *Handbook of X-ray Photoelectron Spectroscopy,* published by Perkin-Elmer Corporation Physical Electronics Division 6509 Flying Cloud Drive Eden Prairie, MinnCSOla 55344 United States of America, (1992).

62 Wang X, Yang W, Li F, Xue Y, Liu R & Hao Y, *Ind Eng Chem Res*, 52 (2013) 17140.

63 Fouda A S, NazeerA A& El behairy W T, *J Bio Tribo Corros*, 4(2018) 7.

64 Boumhara K, Tabyaoui M, Jama C & Bentiss F, *J Ind Eng Chem*, 29 (2015) 146.

65 Singh P, Srivastava V & Quraishi M A, *J Mol Liq*, 216 (2016) 164.